

<http://dx.doi.org/10.35630/2199-885X/2020/10/3.32>

MORPHOLOGY OF FACIAL SKELETON IN CHILDREN WITH UNDIFFERENTIATED CONNECTIVE TISSUE DYSPLASIA

Received 15 July 2020;
Received in revised form 28 August 2020;
Accepted 1 September 2020

Vazgen Avanisyan¹ , Ghamdan Al-Harazi²,
Tatyana Kondratyeva¹ , Yuri Harutyunyan¹,
Dmitry Domenyuk¹ , Sergei Dmitrienko³ ,
Stanislav Domenyuk⁴ 

¹ Department of General Practice Dentistry and Child Dentistry, Stavropol State Medical University, Stavropol, Russia

² Department of Orthodontics, Pedodontic and Preventive Dentistry, Faculty of Dentistry, Sana'a University, Yemen

³ Department of Dentistry, Volgograd State Medical University, Volgograd, Russia

⁴ North Caucasus Federal University, Stavropol, Russia

✉ domenyuka@mail.ru

ABSTRACT — In order to determine the major cephalometric and gnathometric features in children with undifferentiated connective tissue dysplasia, a comprehensive clinical-instrumental and X-ray examination was carried out involving 109 children aged 11–16 and featuring a set of signs pointing at connective tissue failure. Depending on the severity of the external phenotypic manifestations as well as clinical and instrumental signs, the patients were divided into groups with mild, moderate and severe undifferentiated dysplasia. The gnathometric and biometric maxillofacial studies were performed employing traditional methods, while the diagnosis was set following the generally accepted classifications.

The head telereöntgenograms (lateral projection) interpretation was performed in the Dolphin imaging software. The analysis of the head telereöntgenograms (lateral projection) was done through the Schwartz S. method subject to the norm indicators proposed by A. A. Anikienko. The nature and the intensity of morphofunctional issues in the craniofacial structures (small stigmas) were found to be determined by the severity of dysplastic connective tissue disorders.

Constitutional and morphological dysgenesis, as a manifestation of connective tissue dysplasia, is the reason behind abnormal development in the anatomical structure of the cranial and facial regions. It is displayed through increasing dolichocephaly with a decrease in the face width and vertical size, poorly developed jaws, distal displacement of the mandible in relation to the skull base combined with a deep incisal overbite, increased sagittal interincisal distance, and the vertical type of jaw growth. Thus, the pathogenetic mechanisms facilitate the development of malocclusions.

KEYWORDS — children, adolescents, undifferentiated connective tissue dysplasia, facial skeleton, cephalometry, gnathometry, maxillofacial region, lateral projection of head telereöntgenogram.

INTRODUCTION

Nowadays, researchers and clinicians are particularly interested in studying the pathogenesis, clinical polymorphism, and hereditary connective tissue diseases, as well as in developing and improving advanced techniques for their diagnosis and pathogenetic treatment [2, 26, 41].

Connective tissue dysplasia (CTD) is a genetically determined condition that features issues in the fibrous structures and in the connective tissue main substance, which leads to disturbed development of organs and systems, and which has a proгредиant course determining associated pathologies' specifics, as well as the respective medicine pharmacokinetics and pharmacodynamics [4, 7, 30, 39].

CTD development is based on inherited mutations of genes encoding the synthesis and spatial arrangement of collagen, structuring proteins and protein-carbohydrate combinations, as well as mutations of enzyme genes and respective cofactors. From the morphological aspect, these changes reveal improper development of collagen chains, resulting in abnormal collagen trimmers that are unstable to mechanical loads, while elastic fibrils, glycoproteins and proteoglycans with fibroblasts are also subject to irreversible change [5, 29, 47].

CTD clinical manifestations depend on the predominance of lesions in the dense or loose connective tissue, the number and quality of mutations, the nature and severity of fibrillogenesis disturbance. Due to the common presence of connective tissue (skin, bones, cartilage, vascular walls, organs stroma), the disease features a polysystemic nature and a variety of symptoms [3, 6, 8, 27].

Connective tissue, which accounts for 50 to 80% of the body weight, carries vital functions (trophic, plastic, barrier, biomechanical, morphogenetic), determines the morphofunctional integrity of the macroorganism, and responds to almost any pathological and physiological effect. The maxillofacial region features a complex anatomical structure, a large number of involved tissues, and their specific interaction. Embryogenesis and postnatal transformations of the dental apparatus help understand the mechanisms behind dysmorphia development, which is based on an inherited or acquired defect of connective tissue,

and offer a clear confirmation to the dominant shaping role of mesenchymal tissue and its integrating function. Disturbed development of connective tissue is the predetermining factor to dysmorphia involving all types of tissues that make up the organs in the maxillofacial region [1, 25, 31, 40].

The structural and functional components of connective tissue are involved actively in inflammatory, destructive and protective processes in various acute and chronic pathological conditions. Diagnostic dental markers for undifferentiated CTD include anthropometric features of the facial skeleton, dental issues, dental caries, periodontopathy, temporomandibular joint dysfunction, altered oral mucosa, oral cavity small vestibule, congenital short tongue frenulum, and narrowing lower jaw [10, 12, 20, 22–24, 43].

The current stage of development of certain divisions within clinical dentistry shows a significant increase in the role of anthropometric, morphological, genetic and functional research methods when it comes to solving the most urgent problems [11, 13–19, 21, 28, 42].

The priority task that clinicians are facing in view of the current demands implies improving the quality of criteria indicators, better treatment and diagnostic measures and protocols for follow-up cases with dental issues while relying upon principles of personalized medicine, as well as achieving sustainable long-term outcomes of dental treatment and improving patient quality of life [9, 32–38, 44–46].

Despite a significant number of respective research items, the data on the facial skeleton structure in children with CTD remains scattered. Given that, it appears relevant to study diagnostically significant gnathometric and cephalometric indicators in children with CTD of various severity, which would allow forming groups with a high risk of developing a multisystem pathology, as well as improving treatment methods for maxillofacial issues.

Aim of study:

to identify the major cephalometric and gnathometric features in children with undifferentiated CTD, which contribute to development of malocclusions

MATERIALS AND METHODS

Prior to clinical radiological studies involving children, independent informed consent was obtained from their parents.

The work itself implied a set of clinical, paraclinical and laboratory studies involving 109 children (62 girls, 47 boys) aged 11–16, with general somatic pathology, as well as CTD symptoms, who were treated at the Filippky Pediatric Hospital (Stavropol,

Russia). CTD diagnostics was performed following a unified diagnostic algorithm, involving doctors of related specialties. This was important in order to detect details of the lesions affecting organs and systems in this category of children. After excluding differentiated dysplasia with distinct clinical manifestations and detected inheritance (Marfan syndrome, Ehlers–Danlos syndrome, osteogenesis imperfecta, Stickler syndrome), CTD diagnostics included the following symptoms: at least six external phenotypes; multi-organ and multisystem distribution of pathological processes; signs of familial accumulation of collagenopathies; biochemically and immunohistochemically proven disorders of connective tissue metabolism.

The assessment of the CTD severity, depending on the external phenotypic manifestations and laboratory, clinical and instrumental signs, was performed in accordance with the recommendations by L.N. Abbakumova, T.I. Kadurina (2008). Taking into account the external phenotypic signs, as well as laboratory data and clinical examinations, CTD of the mild degree (scores below 30); the medium degree means a score of 30–44, while a score of 45 or above corresponds to the severe degree of CTD. The final diagnosis of CTD took into account the diagnostic tables for the CHILD category in cases where the diagnostic level of +70 was exceeded (E. P. Timofeeva, 1996). Based on the research outcomes, the patients were divided into three subgroups: Subgroup 1 — mild degree of CTD (n=31); Subgroup 2 — medium degree of CTD (n=37); Subgroup 3 — severe degree of CTD (n=41). The control group included 47 children belonging to health groups I and II (Yu.E. Veltischev, 1994), comparable in age and gender.

The diagnostics of dental anomalies relied on the results of clinical examinations, which included medical background evaluation, general examination of the face: symmetry, proportions in the jaw development, the lips position, the severity of nasolabial and chin folds, the degree of mouth opening, and the breathing type. The oral cavity examination included assessing the teeth and periodontium hard tissues status, the teeth position in the dental arch, the dentition shape and size, as well as their ratios. The orthodontic diagnosis was made on the basis of commonly accepted classifications. When making a preliminary diagnosis, we employed the Angle morphological classification, while the final diagnosis was based on the occlusion anomalies classification (Moscow State University of Medicine and Dentistry; 1990) as well as the occlusion anomalies classification by L.S. Persin (1989), recommended by the Resolution of the X Congress of the Professional Society of Russian Orthodontists (2006) as a single classification for orthodontic, surgical and

orthopedic clinics.

The identification of cephalometric indicators included linear and angular measurements of the head and face, along with assessing the head longitudinal and transverse diameter, the face morphological height, the zygomatic diameter, the head index, the facial index, the facial angle, and the nasal index using the conventional Martin and Garson methods.

After placing the head in the Frankfort horizontal, the following cephalometric measurements were performed: *eu-eu* — the head transverse diameter; *g-op* — the head longitudinal diameter; *n-gn* — the face morphological height; *zy-zy* — the face zygomatic diameter. The Garson facial index was identified based on the face morphological height ratio (*n-gn*) to the face width at the zygomatic arches (*zy-zy*). This index was employed to identify the following types of the face: hyperurisopic (<79.9%); euriprosopic (80.0–84.5%); mesoprosopic (85.0–89.9%); leptiprosopic (90.0–94.9%); hyperleptiprosopic (>95.0%). An equally important value in the facial skull is the facial angle, which is shaped through crossing of the line connecting the prosthion (pr) with the nasion (n) and the auricular (Frankfort) horizontal. Depending on the facial angle, the following types of facial skull can be identified: prognathic (70.0–79.9°); mesognathic (80.0–84.9°); orthognathic (85.0–92.9°); hyperorthognathic (>93.0°). Based on the head indicator — the ration of the transverse and longitudinal diameter of the cerebral part of the head, the following craniotypes were identified: dolichocephaly (<75.9); mesocephaly (76.0–80.9); brachycephaly (81.0–85.4); hyperbrachycephaly (>85.5). In anthropometry of the face soft parts, the measurement of the nasal area is of key value. The nasal index was calculated as a ration between the nose width (the greatest distance between the outer points of the piriform opening, or the nose wings) to the nose height (the distance between the upper nasal and the sub-spinal points).

As for the X-ray diagnostics methods, orthopantomography (Fig. 1a) and telereöntgenography of the head (lateral projection) (Fig. 1b) were used on a cone-beam Planmeca ProMax^{3D} Plus computer tomograph with cephalostat (Planmeca). The data was processed using the Romexis Viewer software package, which allows obtaining, processing, storing, and exporting 2D and 3D images in the conventionally accepted medical formats DICOM.

The interpretation of the head telereöntgenograms (lateral projection) was performed in the Dolphin imaging software (USA); the indicators that determine the distal occlusion (Schwartz S.) were studied (Fig. 2).

The lateral projection of the head telereöntgenograms obtained from children with CTD was used

to study linear and angular parameters describing the jaw bones position in the skull space. The analysis of the obtained data was carried out according to the method proposed by Schwartz S. (1955) and employment of the indicators for a norm by Anikienko A.A. (2014).

Studying the linear parameters: **N-A** — the line between points N and A; **N-B** — the line between points N and B; **N-Se** — the length of the skull base anterior segment; **NL** — the plane of the upper jaw base (through Sna and Snp); **NSL** — the line of the anterior skull base, used to measure angular dimensions (continuation of the **NS line**); **H** — the line from the **Or** point to the **C** point; **MP** — the plane of the mandible base; **MP₁** — the tangent to the mandible lower contour; **MP₂** — the tangent to the rear contour of the lower jaw branches; **Pn** — the nasal plane, the plumb line perpendicular to the plane of the skull base front; **OcP** — the occlusal plane dividing the middle of the incisal crossbite and the contacting last teeth tubercle crossbite; **i-I** — the longitudinal axis of the upper central incisor passing through the middle of the tooth apex and canal; **i-I** — the longitudinal axis of lower central incisor passing through the middle of the tooth apex and canal.

Studying the angular parameters: **<SNA** — the angle that describes the position of the upper jaw in the sagittal plane; **<SNB** — the angle, which describes the position of the mandible in the sagittal plane; **<NScAr** — the angle describing the position of the mandible head in the sagittal direction; **<ScArGo** — the angle, which describes the position of the lower jaw branches in the sagittal direction; **<ArGoMe** — the angle describing the relative positions of the mandible body and branch; **<NSE-SpP** — the angle, which describes the upper jaw slope towards the skull anterior base; **<NSE-MP** — the angle, which describes the mandible body slope to the skull anterior base; the **basal B angle** is the inclination angle of the jaws base to each other (**SpP-MP**), which offers a description of the jaws vertical position; the inclination angle of **Axis 1** to **SpP**; the inclination angle of **Axis I** to **MP**; the interincisal angle **ii** is shaped by the intersection of the long axes of the upper and lower incisors and determines their relative positions; **<NSE-OcP** — the inclination angle of the occlusal plane to the skull base. **The mandibular G angle** is located between the tangent to the mandible lower edge (**MT₁**) and the rear surface of the mandible branches (**MT₂**); the mandible body length (**MT**) — from the projection of the Pg point onto **MP** to the point of its intersection with the tangent to the mandible branch on the **MP** plane; **the maxilla length** — from the intersection point of the perpendicular from the **A** point to **SpP**, up to the **Sn**

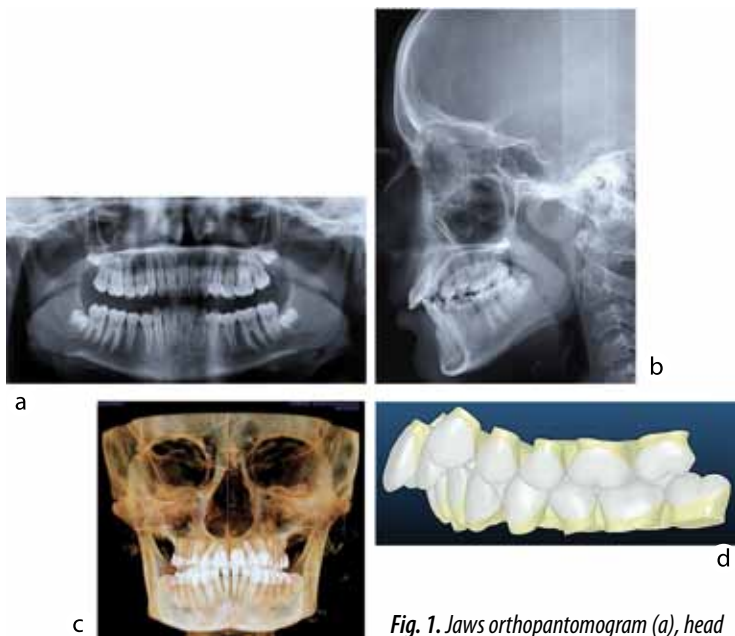


Fig. 1. Jaws orthopantomogram (a), head telereöntgenogram (lateral projection) (b), 3D panorama at FOV 8×15 in Unshaded VR mode (frontal projection) (c) and virtual diagnostic Set-Up model in the file "ORAPIX" 3Txe 2.5.0 (Japan) (d); patient T with CTD, 16 y.o.

point; **the mandible branch height** — the tangent to the branch rear edge from the point of intersection with the MP plane to the C point projection on the tangent; **the sagittal interincisal distance** goes parallel to the Frankfort horizontal between the cutting edges of the upper and lower central incisors; **the incisal overlap depth** — the distance between the projections of the central upper and lower incisors cutting edges on the Pn nasal plane; **the face anterior height** — the interval between the projections of points N and Me, where the point SNA breaks it into the upper (N-SNA) and the lower (SNA-Me) parts; \angle NSeAr — the angle, which describes the position of the mandible head in the sagittal direction; \angle SeArGo — the angle that describes the position of the mandible branches in the sagittal direction; \angle ArGoMe — the angle that describes the relative position of the mandible body and branches. The neutral, horizontal or vertical growth types of the skull facial part in children with distal occlusion were identified by the total Bjork angle — the sum of the three angles (\angle NSeAr, \angle SeArGo, \angle ArGoMe).

For teeth and dentition biometric measurements, diagnostic cast models of the jaws were used (Fig. 3).

When identifying the width of the teeth crown part, the reference was the mesiodistal dimension at the equator area, the exception being the lower incisors, where reference point was the cutting edge. The obtained morphometric outcomes were evaluated in view of individual facial features and their relationship with the odontometric indicators. The proportionality of the permanent incisors width in the lower and upper jaws was calculated using the Tonn

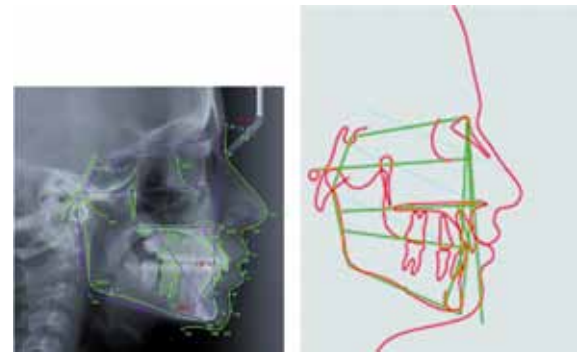


Fig. 2. Head telereöntgenogram analysis (lateral projection), Dolphin imaging software (USA)

and Bolton method. The palate height measurements were based on the index of the palate height index (Persii L.S., 2003). Another value identified was the ratio between the sum of the mesiodistal dimensions of 14 permanent teeth and the diagonal dimensions of the face and the dental arches.

The statistical processing of the obtained data was performed using the SPSS 21.0 software package and methods of variation statistics in Microsoft Excel, adjusted to biomedical research.

RESULTS AND DISCUSSION

The orthognathic bite was detected in 23 children with CTD (the main group) (21.1%). As for the phenotypic signs of the dental system (small stigmas) in children with CTD, the following were detected: narrowed and deformed dental arches — 79 children (72.5%); deformed occlusal Spee curve — 74 children (67.9%); "Gothic" or "arched" palate — 69 children (63.3%); abnormal attachment of the lips and tongue frenulum, true diastema — 66 children (60.6%). Of the pathological bites, the most common were distal and deep incisional occlusion — 81 children (74.3%). Children with CTD who had occlusion pathology, featured a history of early loss of baby teeth, which contributes to the development of dental and speech issues, as well as to a disturbed chewing efficiency. Deviated nasal septum, which was diagnosed in 63 children (57.8%), as well as the growth of lymphoid tissue in



Fig. 3. Diagnostic cast models of jaws, patient S. with CTD, 17 y.o.; lateral right (a), frontal (b) and lateral left (c) projections: prognathic bite, skeletal form, complicated by open bite; distal occlusion. Sagittal inter-incisal distance is increased; narrowed and deformed dentition; lower jaw front teeth — crowded, with mesial position; protruded upper jaw incisors

the nasopharynx, was a predisposing factor behind oral or mixed type of breathing.

The distribution of children in the study groups by type of facial skull (facial index) is shown in Table 1.

The evaluation of the facial skull type with a facial index revealed that the greatest share of patients with moderate and severe degrees of CTD had leptoprosopic and hyperleptoprosopic shapes, while the children in health groups I and II, as well as children with a mild degree of CTD had the mesoprosopic and leptoprosopic face types prevailing.

Table 2 offers a view at the distribution of the children within the groups following the facial skull (facial angle).

Evaluating the facial skull using the facial angle indicator revealed that the orthognathic and mesognathic skull types dominated in all the cases within the groups, while there were no statistically significant differences to be observed among the groups.

Table 3 shows the distribution of the patients based on the skull shape (cephalic index).

The craniotype assessment based on the cephalic index showed that the largest number of patients with moderate and severe CTD featured the dolichocephalic type, while the children belonging to health groups I and II, as well as the children with mild CTD, had an even distribution across the craniotypes.

The major cephalometric features of the children within the groups can be seen from Table 4.

An analysis of the average values for the main cephalometric indicators allowed detecting statistically significant differences among the parameters within the groups for further identification of the direction vector in the maxillofacial changes. An increase in the facial index values from the mild to the severe degree of CTD was indicative of a growing dynamics of

latitudinal indicators decreasing towards the narrow face in children within subgroup 3. The decreasing dynamics for the cephalic index changes along with an increase in the CTD severity reflected the nature of the sign displacement towards the dolichocephalic head shape (dolichocephalization) in the children featuring a severe degree of CTD. The positive tendency towards an increase in the nasal index with progressing mesenchymal dysplasia reflected the dynamics of decreasing face vertical size within subgroup 3 of the main group. The lack of statistically significant differences among the facial angle size features in the groups points at the dominance of the mesognathic (facial angle — 80–84.9°) and the orthognathic (facial angle — 85° or above) types of facial skull with a vertical profile.

A comparative evaluation of the cephalometric parameters within the studied groups showed that the children with CTD, in contrast to the children in health groups I and II, had morphological changes in the maxillofacial area. The change direction vector in the facial and cephalic parts of the skull was towards hypoplastic variants (trends), while the child's body development rate through the postnatal period could be called slow (*retardatio*), due to later anlage of organs. The nature of the detected changes (dolichocephalic; hypoplastic variants of the head facial and cephalic structure; skeletal abnormalities in the maxillofacial area) were the result of a genetically determined set of anatomical, constitutional, dysplastic internal and external phenotypic features.

Table 5 contains gnathometric indicators within the groups.

An analysis of gnathometric parameters in patients with moderate and severe degrees of CTD revealed the following morphological features in the

Table 1. Distribution of patients based on the type of facial skull (facial index)

Facial Skull Type	Research groups			
	Main group 1 st subgroup, n=31	Main group 2 nd subgroup, n=37	Main group 3 rd subgroup, n=41	Control group, n=47
Hyperevipsopic Type	1 (3,2%)	0 (0%)	0 (0%)	1 (2,1%)
Evipsopic Type	2 (6,4%)	1 (2,7%)	1 (2,4%)	2 (4,2%)
Mesoprosopic Type	17 (54,8%)	3 (8,1%)	2 (4,8%)	34 (72,3%)
Leptoprosopic Type	8 (25,9%)	22 (59,5%)	25 (60,9%)	8 (17,2%)
Hyperleptoprosopic Type	3 (9,7%)	11 (29,7%)	13 (31,9%)	2 (4,2%)

Table 2. Distribution of patients based on the type of facial skull (facial angle)

Facial Skull Type	Research groups			
	Main group 1 st subgroup, n=31	Main group 2 nd subgroup, n=37	Main group 3 rd subgroup, n=41	Control group, n=47
Prognathic Type	2 (6,4%)	3 (8,1%)	3 (7,3%)	3 (6,4%)
Mesognathic Type	8 (25,9%)	7 (18,9%)	11 (26,8%)	12 (25,5%)
Orthognathic Type	19 (61,3%)	23 (62,2%)	25 (61,1%)	28 (59,6%)
Hyperorthognathic Type	2 (6,4%)	4 (10,8%)	2 (4,8%)	4 (8,5%)

Table 3. Distribution of patients based on the craniotype (cephalic index)

Skull shape	Research groups			
	Main group 1 st subgroup, n=31	Main group 2 nd subgroup, n=37	Main group 3 rd subgroup, n=41	Control group, n=47
Dolichocephalic Type	10 (32,2%)	26 (70,3%)	30 (73,2%)	14 (29,8%)
Mesocephalic Type	12 (38,7%)	5 (21,6%)	9 (21,9%)	15 (31,9%)
Brachycephalic Type	9 (29,1%)	3 (8,1%)	2 (4,9%)	18 (38,3%)

Table 4. Cephalometric parameters in the groups, ($M \pm m$)

Research indicators	Research groups			
	Main group 1 st subgroup, n=31	Main group 2 nd subgroup, n=37	Main group 3 rd subgroup, n=41	Control group, n=47
Face index	87,9 \pm 0,98*	89,4 \pm 0,96*	92,6 \pm 1,17*	86,9 \pm 0,84
Head index	80,5 \pm 0,31*	77,4 \pm 0,23*	72,3 \pm 0,28*	80,8 \pm 0,27
Nasal index	53,1 \pm 0,77*	53,9 \pm 0,79*	55,7 \pm 0,74*	52,8 \pm 0,72
Face angle	86,6 \pm 0,83*	85,7 \pm 0,79*	86,1 \pm 0,71*	85,1 \pm 0,74

Note. * — $p \leq 0.05$ statistically significant in comparison with the parameters of patients in the control group, (Wilcoxon's T-test).

facial skeleton: the maxilla, if taken in relation to the cranial base, has the right position, being rather horizontal; the mandible, if taken in relation to the cranial base, features some distal displacement, while it is inclined downwards in the vertical plane, which points at the vertical growth of the jaws; the maxillary (basal)

angle, as well as the lower jaw angle, is enlarged; the upper incisors, viewed in relation to the jaw base, have a vestibular inclination; the lower incisors, in relation to the jaw base, have an oral inclination; the interincisal angle is reduced; the occlusal plane has a tilt down toward the skull base; the anterior face height is reduced;

Table 5. Gnathometric indicators in the groups, ($M \pm m$)

Indicators, units	Research groups			
	Main group 1 st subgroup, n=31	Main group 2 nd subgroup, n=37	Main group 3 rd subgroup, n=41	Control group, n=47
Upper jaw length, mm	50,9 ± 0,67*	43,6 ± 0,49*	44,3 ± 0,41*	51,3 ± 0,56
Lower jaw length, mm	66,7 ± 0,78*	59,9 ± 0,42*	59,6 ± 0,49*	67,4 ± 0,81
Lower jaw branch height, mm	59,3 ± 0,64*	52,2 ± 0,51*	51,9 ± 0,73*	60,5 ± 0,77
Sagittal inter-incisal distance, mm	4,3 ± 0,08*	7,6 ± 0,14*	9,1 ± 0,19*	3,2 ± 0,05
Depth of incisal overlap, mm	3,6 ± 0,07*	6,5 ± 0,13*	7,3 ± 0,14*	2,9 ± 0,09
Front face height, mm	112,6 ± 1,79*	107,6 ± 1,23*	105,9 ± 1,74*	113,2 ± 2,03
<SNB	79,1 ± 0,66*	75,2 ± 0,81*	73,3 ± 0,72*	79,9 ± 0,94
<SNA	81,3 ± 0,48*	82,1 ± 0,74*	81,5 ± 0,71*	81,8 ± 0,68
<NSE - SpP	7,7 ± 0,11*	7,3 ± 0,12*	7,0 ± 0,17*	8,2 ± 0,18
<NSE - MP	31,4 ± 0,19*	37,1 ± 0,12*	37,9 ± 0,23*	32,5 ± 0,21
<SpP - MP	26,9 ± 0,12*	32,3 ± 0,19*	34,5 ± 0,23*	26,3 ± 0,17
<I - SpP	81,9 ± 1,24*	73,4 ± 1,06*	73,9 ± 0,97*	80,3 ± 1,19
<I - MP	95,2 ± 1,22*	87,8 ± 1,19*	87,4 ± 1,07*	94,8 ± 1,27
<i - i	128,9 ± 1,25*	120,6 ± 1,17*	119,2 ± 1,19*	129,9 ± 1,18
<NSE - OcP	17,6 ± 0,14*	22,1 ± 0,31*	24,9 ± 0,16*	16,9 ± 0,18
<MT1 - MT2	125,7 ± 0,73*	129,7 ± 0,85*	128,5 ± 0,89*	126,1 ± 0,84

Note. * — $p \leq 0.05$ statistically significant in comparison with the parameters of patients in the control group, (Wilcoxon's T-test).

the upper and the lower jaws, as well as the lower jaw branch, are reduced in size; the cutting depth of the incisal crossbite is increased; the sagittal interincisal distance is increased (Fig. 4–5).

Children with a mild degree of CTD feature cephalometric and gnathometric indicators that fall within the average standard values, except for a small increase in the incisal crossbite and sagittal interincisal distance, as well as an increase in the upper incisors inclination towards the jaw base, and a decrease in the interincisal angle (Fig. 6).

Dolichocephalism processes in children with CTD, if compared to healthy children, is confirmed with the side teleroentgenograms of the head: prevalence of the vertical facial skeleton growth over the horizontal and neutral (the ratio between the posterior and the anterior heights of the face — $SGo/NMe=56-50\%$; hyperdiverging type — a too obtuse NSBa angle (the skull base angle); increased maxillary angle parameters $<NL-ML=33-43^\circ$; increased angle of the mandible body base plane to the anterior skull base — $<ML-NSL=37-47^\circ$; increased lower genial angle $<NGoMe=78-86^\circ$; decrease in the Ricketts facial angle — $<NBa-PtGn=87-81^\circ$; the total Bjork angle — $<NSAr + SArGo + ArGoMe=401-411^\circ$); a convex facial profile due to disproportionate total of the facial skeleton heights; a short narrow mandible branch; the upper jaw moved forward and downward;

reduced dimensional values of the lower dentition apical basis, mandible body, as well as the height and the width of the mandible branches; deepening notch on the outer edge of the mandible body; elongated and thinned symphysis; lack of the cortical layer at the Gn point (Fig. 2 a–e).

An analysis of anthropometric parameters in the facial area the head, the jaw bones, the teeth and dentition in children with CTD has helped identify the following skeletal issues in the facial skull: a distal shift of the mandible in relation to the cranial base, combined with a deep incisal crossbite; poorly developed upper, lower jaws; increased sagittal interincisal distance and the vertical type of jaw growth, which causes a truly prognathic ratio in the jaw bones; deformed and narrowing dental arches; mesial displacement (position) of the teeth; crowded teeth. Note to be made that the intensity of the dentofacial structure changes reveals a correlation with the number of CTD phenotypic manifestations, while the degree of organs and systems involvement in the dysplastic process features a direct relation with the severity of connective tissue disorders.

Based on the lateral projection of the head TRG, the children in health groups I and II, if compared with the main group, had a smoother face profile, their lower jaw being moderately developed, the body of the lower jaw more horizontal, its branches wide, and

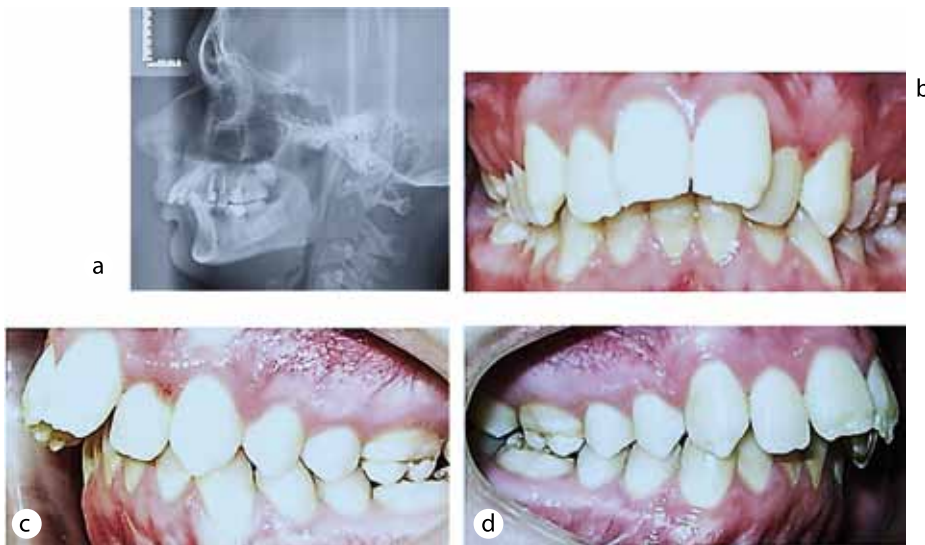


Fig. 4. X-ray and photographic features of dental system, patient M., 15 y.o., with severe CTD. Head telereöntgenogram, lateral projection (a), pathological occlusion (b — direct projection, c — left-side lateral projection, d — right-side lateral projection)

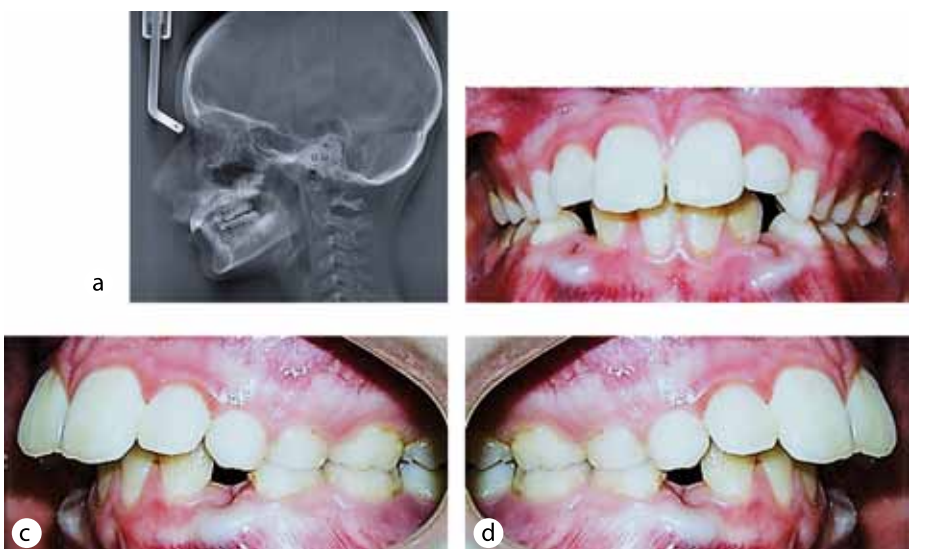


Fig. 5. X-ray and photographic features of dental system, patient A., 11 y.o., with moderate CTD. Head telereöntgenogram, lateral projection (a), pathological occlusion (b — direct projection, c — left-side lateral projection, d — right-side lateral projection)

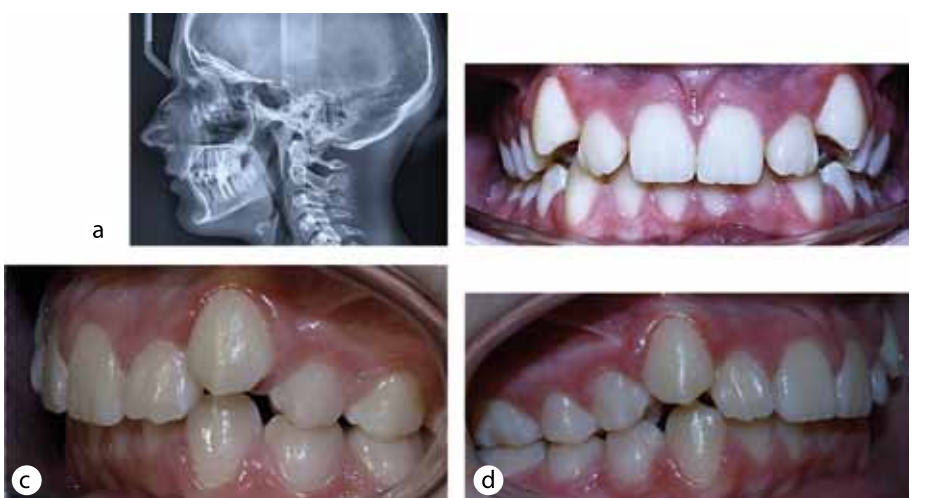


Fig. 6. X-ray and photographic features of dental system, patient S., 14 y.o., with mild CTD. Head telereöntgenogram, lateral projection (a), pathological occlusion (b — direct projection, c — left-side lateral projection, d — right-side lateral projection).

the height of the mandible not disturbed. At the Gn point, the cortical layer is expressed significantly, while the mandibular symphysis is wide and short. Children in the comparison group, talking of the neutral facial skeleton type dominating over the vertical one, had the following signs: increased ratio of the front and rear height of the face — $SGo/NMe=62-65\%$; decreased maxillary angle $<NL-ML=25-31^\circ$; reduced angle of the mandible base body plane to the anterior skull base — $<ML-NSL=29-35^\circ$; reduced lower genial angle — $<NGoMe=70-76^\circ$; increased Ricketts facial angle — $<NBa-PrGn=92-89^\circ$; a decrease in the total Bjork angle — $<NSAr + SArGo + ArGoMe=393-399^\circ$ (Fig. 7).

(size, length) of apical basis on both jaws. We believe that the lack of consistency between the jaw bones parameters (shortened and narrowed) with the teeth size (large, elongated) is due to a higher rate of the jaws reduction (upper, lower) prevailing over not so intensive rate of the teeth reduction.

In case of CTD, there is a close relationship between the number of external phenotypic signs (big, small stigmas) and the internal organs pathology, while the functional failure of connective tissue in the organs and systems, which progresses over age, works an inducing effect on the acquired diseases course, thus contributing to early manifestations. This means

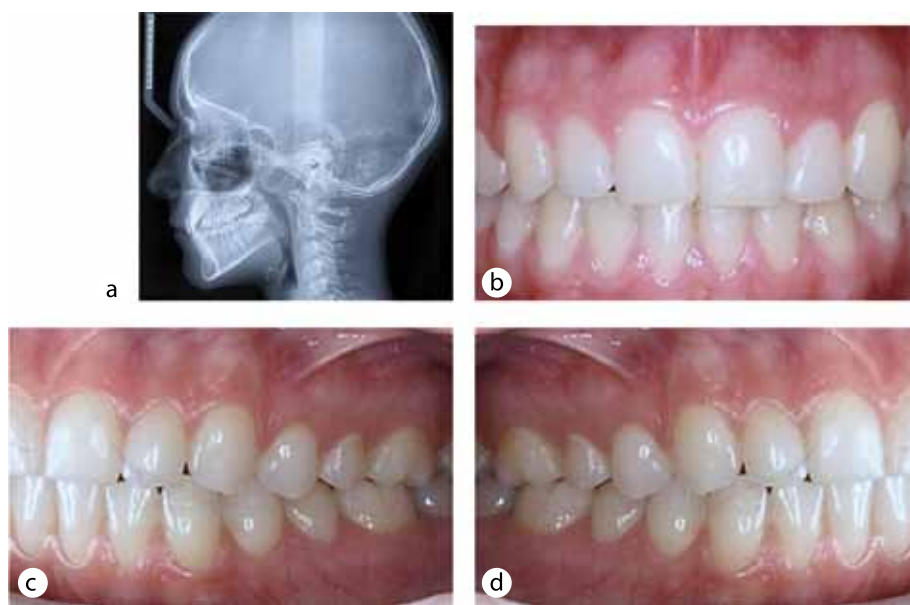


Fig. 7. X-ray and photographic features of dental system, healthy patient K., 16 y.o. Head telereöntgenogram, lateral projection (a), physiological occlusion (b — direct projection, c — left-side lateral projection, d — right-side lateral projection)

The available research data, as well as the outcomes of our own study, allow claiming that there are other pathomorphological signs that are of value in terms of the clinical, diagnostic and prognostic value when we have to deal with external phenotypic manifestations (small stigmas) involving the dentition in patients with CTD featuring permanent teeth bite: increased odontometric parameters of the crown; vestibule-oral lengthening of the teeth crowns in the upper (central incisors, canines, first molars) and in the lower (incisors, canines) jaw; hypomineralized tooth enamel and dentin; pointed, elongated and protruded teeth roots; denticles found in teeth cavities; contracted root canals; enamel hypoplasia of varying severity; elongated front (limited to canines) part of the dental arches on both jaws; decreased width of the dental arches at the level of the first molars and premolars on both jaws; a decrease in the morphological parameters

that underestimating the role of CTD leads to delayed identification of key prognostic conditions, increased risk of developing general somatic complications, insufficient comprehensive prevention measures, improper rehabilitation and management tactics applied to such patients, which finally affects the health of the child population suffering from connective tissue dysplasia.

CONCLUSIONS

1. To improve the algorithm for diagnosing undifferentiated CTD types in children at the first appointment, we have systematized diagnostically significant signs (small stigmas), which determine the morphology of the craniofacial structures: dolichocephaly; hypoplastic types of the facial and cephalic head parts; skeletal anomalies of the maxillofacial area; narrowed and deformed dental arches; a deformed occlusal *Spee* curve; “Gothic”

- or “arched” palate; abnormal lips and tongue frenulum attachment, true diastema; distal and deep incisal occlusion.
2. Constitutional and morphological congenital development issues (dysgenesia), viewed as manifestations of the connective tissue failure, are an etiopathogenetic factor behind the developing abnormalities in the facial and cephalic parts of the skull. The nature and intensity of morphological and functional manifestations in the maxillofacial area (phenotypic features, small stigmas) is determined by the severity of connective tissue dysplasia.
 3. The highest number of patients with the moderate and severe degrees of CTD had leptoprosopic, hyperleptoprosopic facial skulls and a dolichocephalic craniotype, while healthy children and children with a mild degree CTD featured the mesoprosopic and leptoprosopic facial skulls prevailing with a uniform distribution within craniotypes.
 4. The vector for the facial and cephalic skull changes in children with CTD, as observed from cephalometric studies, is oriented towards strengthening hypoplastic trends and dolichocephaly. As a proof to this may serve the following: the vertical growth of the facial skeleton dominating over the horizontal and neutral ones; a convex face profile along with disproportionate total heights of the facial skeleton; reduced width parameters and increased height parameters of the face; a short narrow branch of the lower jaw; upper jaw displaced downwards and forward; reduced size of the apical base in the lower dentition, the lower jaw body, as well as in the lower jaw branches height and width; deepening notch on the outer edge of the lower jaw body; elongated and thinned symphysis; lack of cortical layer at the Gn point.
 5. The gnathometric and biometric studies of the maxillofacial area in children with connective tissue failure, which determine dynamic and static occlusion, revealed the following facial skeleton issues: a distal shift of the mandible viewed in relation to the cranial base, combined with a deep incisal crossbite; poorly developed upper and lower jaws; increased interincisal distance along the sagittal, which determines the prognathic ratio of the jaw bones; deformed and narrowed dental arches; a mesial shift (position) of the teeth; crowded teeth; a mismatch between the teeth size and the dental arch parameters in the transversal and sagittal planes; a mismatch between the true sizes of the maxillary bone (width and length) and the forecasted (optimal) one; disproportionate and disturbed dentition.
 6. Given the increased maxillofacial lability and a high predisposition to developing immediate, long-term complications (improper vascular responses, lengthening of bone remodeling and ossification, a tendency to TMJ dysfunction), orthodontic treatment of dentition anomalies in children with CTD should be carried out in view of the short path and small forces in designing the equipment, expanding the indications for trainers, which is due to the oral mucosa and muscle fibers compliance, as well as due to a longer retention period.
 7. In view of connective tissue failure in cases with undifferentiated dysplasias, traditional orthodontic treatments applied to children with dental issues may lead to a relapse, and will not allow getting a stable expected outcome. Medication pathogenetic therapy, as a mandatory component through the entire period of orthodontic treatment, should be of a substitutive nature and include the following parts: correction of the disturbed glycosaminoglycan synthesis; stimulation of collagen synthesis; regulation of redox mechanisms; stabilization of phosphorus-calcium metabolism.
 8. The identified association between certain constitutional and morphological features and CTD has to be taken into account when examining children and adolescents in organized groups thus aiming to develop groups running a high risk of developing general somatic and dental pathologies. It has been proven that along with progressing severity of connective tissue-related dysplastic disorders the prevalence of dental anomalies and deformities increases.
 9. The patient-oriented approach applied through the stages of diagnostics, treatment and rehabilitation of children with CTD should imply close collaboration with dentists, maxillofacial surgeons, pediatricians, therapists, cardiologists, neurologists, ophthalmologists, gastroenterologists. Interdisciplinary collaboration that allows early detection of pathologies associated with CTD, irreversible morphofunctional changes, dysplastics-dependent disorders that may affect the child's life quality, would allow changing the traditional approach and shifting towards personalized diagnostics and differential treatment of this category of patients, in view of their individual features.

REFERENCES

1. **P. B. BAKER, G. BANSAL, K. BOUDOULAS ET AL.** Floppy mitral valve chordae tendineae: histopathologic alterations. *Hum Pathol.* 1988; May;19 (5):507–12. DOI: 10.1016/s0046-8177(88)80195-3.
2. **BEIGHTON P., DE PAEPE A., DANKS D.** 1988. International Nosology of Heritable Disorders of Connective Tissue, Berlin, 1986. *Am J Med Genet* 29:581–594.
3. **BLYAKHMAN, F.** Left ventricular inhomogeneity and the heart's functional reserve // *Cardiac Pumping and Perfusion Engineering* / Ed. by Prof. D. Ghista. – World Scientific Press, 2007. 680 p.
4. **A. F. BRADY.** The Ehlers-Danlos Syndromes, Rare Types. *The American Journal of Medical Genetics Part C Seminars in Medical Genetics.* 2017; Vol.175;1: 70–115. DOI: 10.1002/ajmg.c.31550
5. **CASTORI, M.** A framework for the classification of joint hypermobility and related conditions / M. Castori, B. Tinkle, H. Levy et al. / *American Journal of Medical Genetics. Part C, Seminars in Medical Genetics.* – 2017. – Vol. 175C. – P. 148–157.
6. **CLINCH, J.** Epidemiology of generalized joint laxity (hypermobility) in fourteen-year-old children from the UK a population-based evaluation // J. Clinch, K. Deere, A. Sayers et al. // *Arthritis and rheumatism.* – 2011. – Vol. 63, no. 9. – P. 2819–2827. DOI: 10.1186/1546-0096-10-S1-A107
7. **M. M. COHEN.** *The Child with Multiple Birth Defects.* 2nd. ed. New York, 1997.
8. **COLES, W.** Hypermobility in children / W. Coles, A. Copeman, K. Davies // *Paediatrics and child health.* – 2018. – Vol. 28, no. 2. – P. 50–56. DOI: 10.1016/j.paed.2017.12.001
9. **DAVYDOV B. N.** Applied significance of biometric diagnostics in planning dentistry treatment tactics. *Medical alphabet.* 2020; (12):27–35. <https://doi.org/10.33667/2078-5631-2020-12-27-35>
10. **DAVYDOV B.N.** Anthropometric peculiarities of the maxillofacial region in children with congenital pathology in the period of the brew of the dairy teeth. *Pediatric dentistry and prophylaxis.* 2018; Vol. 17; 2 (65): 5–12. (In Russ.) DOI: 10.25636/PMP.3.2018.2.1.
11. **DAVYDOV B.N.** Methodological approaches in diagnostics of anomalies of form and dimensions of dental arc taking into account individual morphological features. *Medical alphabet.* 2020;(3):12–18. <https://doi.org/10.33667/2078-5631-2020-3-12-18>
12. **DAVYDOV B.N.** Modern possibilities of clinical-laboratory and x-ray research in pre-clinical diagnostics and prediction of the risk of development of periodontal in children with sugar diabetes of the first type. Part I. *Periodontology.* 2018; Vol. 23; 3–23(88): 4–11. DOI:10.25636/PMP.1.2018.3.1
13. **DAVYDOV B.N.** Morphological peculiarities of facial skelet structure and clinical and diagnostic approaches to the treatment of dental anomalies in children in the period of early change. *Pediatric dentistry and prophylaxis.* 2019; Vol. 19; 1 (69): 26–38. (In Russ.) DOI: 10.33925/1683-3031-2019-19-69-26-38.
14. **DAVYDOV B.N.** Peculiarities of microcirculation in periodont tissues in children of key age groups sufficient type 1 diabetes. Part I. *Periodontology.* 2019; Vol. 24; 1–24(90): 4–10. DOI: 10.25636/PMP.1.2019.1.1
15. **DAVYDOV B.N.** Peculiarities of microcirculation in periodont tissues in children of key age groups sufficient type 1 diabetes. Part II. *Periodontology.* 2019;24(2):108–119. (In Russ.) DOI:10.33925/1683-3759-2019-24-2-108-119
16. **DMITRIENKO S.V.** Analytical approach within cephalometric studies assessment in people with various somatotypes // *Archiv EuroMedica.* 2019. Vol. 9; 3: 103–111. <https://doi.org/10.35630/2199-885X/2019/9/3.29>
17. **DMITRIENKO S.V.** Enhancement of research method for spatial location of temporomandibular elements and maxillary and mandibular medial incisors // *Archiv EuroMedica.* 2019. Vol. 9; 1: 38–44. <https://doi.org/10.35630/2199-885X/2019/9/1/38>
18. **DMITRIENKO S.** Modern x-ray diagnostics potential in studying morphological features of the temporal bone mandibular fossa // *Archiv EuroMedica.* 2020. Vol. 10; 1: 116–125. <https://doi.org/10.35630/2199-885X/2020/10/36>
19. **DOMENYUK D. A.** Anatomical and topographical features of temporomandibular joints in various types of mandibular arches. *Medical News of North Caucasus.* 2019;14(2):363–367. (In Russ.)<http://dx.doi.org/10.14300/mnnc.2019.14089>
20. **DOMENYUK D.A.** Contemporary methodological approaches to diagnosing bone tissue disturbances in children with type 1 diabetes. *Archiv EuroMedica.* 2018; 8(2): 71–81. DOI:10.35630/2199-885x/2018/8/2/71
21. **DOMENYUK D.** Structural arrangement of the temporomandibular joint in view of the constitutional anatomy // *Archiv EuroMedica.* 2020. Vol. 10; 1: 126–136. <https://doi.org/10.35630/2199-885X/2020/10/37>
22. **FISCHEV S.B., PUZDYRYOVA M.N.** Morphological features of dentofacial area in peoples with dental arch issues combined with occlusion anomalies // *Archiv EuroMedica.* 2019. Vol. 9; 1: 162–163. <https://doi.org/10.35630/2199-885X/2019/9/1/162>
23. **FOMIN I.V.** Effect of jaw growth type on dentofacial angle in analyzing lateral telerradiographic images // *Archiv EuroMedica.* 2019. Vol. 9; 1: 136–137. <https://doi.org/10.35630/2199-885X/2019/9/2/136>
24. **FOMIN I.V., IVANOV S.YU.** Efficiency of osseointegration properties manifestation in dental implants with hydroxyapatite plasma coating // *Archiv EuroMedica.* 2019. Vol. 9; 1: 138–139. <https://doi.org/10.35630/2199-885X/2019/9/2/138>
25. **GRAHAME R.** Time to take hypermobility seriously (in adults and children) // *Rheumatology (Oxford).* 2001. Vol. 40 (5): 485–487. DOI: 10.1093/rheumatology/40.5.485.

26. **HALLER, G.** Lack of joint hypermobility increases the risk of surgery in adolescent idiopathic scoliosis / G. Haller, H. Zabriskie, S. Spehar et al. // *Journal of Pediatric Orthopaedics – Part B.* – 2018. – Vol. 27, no. 2: 152–158. DOI: 10.1097/BPB.0000000000000489.
27. **HARUTYUNYAN YU.** Undifferentiated connective tissue dysplasia as a key factor in pathogenesis of maxillofacial disorders in children and adolescents // *Archiv EuroMedica.* 2020. Vol. 10; 2: 83–94. <https://dx.doi.org/10.35630/2199-885X/2020/10/2.24>
28. **IVANYUTA S.O.** Individual-typological variability of structures of the craniofacial area in people with various constitutions // *Entomology and Applied Science Letters.* 2020. Vol. 7; 1: 20–32.
29. Joint hypermobility syndrome in childhood. A not so benign multisystem disorder? / Adib N., Davies K., Grahame R., et al. // *Rheumatology (Oxford)*, 2005. Vol. 44(6). P. 744–750. DOI: 10.1186/1748-7161-7-S1-O69
30. **T. I. KADURINA, S. F. GNUSAEV, L. N. ABBAKUMOVA ET AL.** Hereditary and multivariate connective tissue disorders in children. Algorithm of diagnosis. Management tactics draft russian recommendations developed by the expert committee of pediatric group «connective tissue dysplasia» at the russian scientific society of phys. *Medical Bulletin of the North Caucasus.* 2015; Vol. 10; 1: 5–35. (In Russ.). DOI: 10.14300/mnnc.2015.10001.
31. **KALLENBERG C.G.** Overlapping syndromes, undifferentiated connective tissue disease, and other fibrosing conditions. *Curr Opin Rheumatol* 1995; 7(6): 568–73. <http://dx.doi.org/10.1097/00002281-199511000-00017>
32. **KONDRATYEVA T.** Methodological approaches to dental arch morphology studying // *Archiv EuroMedica.* 2020. Vol. 10; 2: 95–100. <https://dx.doi.org/10.35630/2199-885X/2020/10/2.25>
33. **KOROBKEEV A. A.** Variability of odontometric indices in the aspect of sexual dimorphism. *Medical News of North Caucasus.* 2019; 14(1.1): 103–107. (In Russ.) <https://doi.org/10.14300/mnnc.2019.14062>
34. **KOROBKEEV A.A.** Types of facial heart depth in physiological occlusion. // *Medical news of North Caucasus.* 2018. – Vol. 13. (4) : 627–630. (In Russ., English abstract). <https://doi.org/10.14300/mnnc.2018.13122>.
35. **KOROBKEEV A.A.** Anatomical features of the interdependence of the basic parameters of the dental arches of the upper and lower jaws of man. *Medical news of North Caucasus.* 2018. – Vol. 13; 1–1: 66–69. (In Russ., English abstract). DOI – <https://doi.org/10.14300/mnnc.2018.13019>
36. **KOROBKEEV A. A.** Clinical and computer-tomographic diagnostics of the individual position of medial cutters in people with physiological occlusion. *Medical News of North Caucasus.* 2020; 15(1): 97–102. (In Russ.) <https://doi.org/10.14300/mnnc.2020.15023>
37. **LEPILIN A.V., FOMIN I.V.** Diagnostic value of cephalometric parameters at graphic reproduction of tooth dental arches in primary teeth occlusion // *Archiv EuroMedica.* 2018. Vol. 8; 37–38. DOI: 10.35630/2199-885X/2018/8/1/37
38. **LEPILIN A.V.** Dependence of stress strain of dental hard tissues and periodontal on horizontal deformation degree // *Archiv EuroMedica.* 2019. Vol. 9; 1: 173–174. <https://doi.org/10.35630/2199-885X/2019/9/1/173>
39. **F. MALFAIT.** The 2017 International Classification of the Ehlers-Danlos Syndromes. *The American Journal of Medical Genetics Part C Seminars in Medical Genetics.* 2017; Vol. 175; 1: 8–26. DOI: 10.1002/ajmg.c.31552
40. **A. I. MARTYNOV, G. I. NECHAEVA, E. V. AKATOVA ET AL.** National recommendations of the Russian scientific society of internal medicine for diagnostics, treatment and rehabilitation of patients with connective tissue dysplasia. *Medical Bulletin of the North Caucasus.* 2016; Vol. 11; 1: 1–76. (In Russ.). DOI: 10.14300/mnnc.2016.11001.
41. **MILEWICZ D.M., URBAN Z., BOYD C.** Genetic disorders of the elastic fiber system. *Matrix Biology* 2000; 19(6): 471–80. DOI: 10.1016/S0945-053X(00)00099-8
42. **PORFYRIADIS M.P.** Scanning electron microscopy and X-ray spectral microanalysis in dental tissue resistance // *Archiv EuroMedica.* 2019. Vol. 9; 1: 177–185. <https://doi.org/10.35630/2199-885X/2019/9/1/177>
43. **PROFFIT W.R., FIELDS H.W.** *Contemporary orthodontics.* - St. Louis: C.V. Mosby, 2000. – 768 p.
44. **SHKARIN V.V., IVANOV S.YU.** Morphological specifics of craniofacial complex in people with varioustypes of facial skeleton growth in case of transversal occlusion anomalie // *Archiv EuroMedica.* 2019. Vol. 9; 2: 5–16. <https://doi.org/10.35630/2199-885X/2019/9/2/5>
45. **SHKARIN V.V., GRININ V.M., KHALFIN R.A.** Specific features of grinder teeth rotation at physiological occlusion of various gnathic dental arches // *Archiv EuroMedica.* 2019. Vol. 9; 2: 168–173. <https://doi.org/10.35630/2199-885X/2019/9/2/168>
46. **SHKARIN V.V., GRININ V.M., KHALFIN R.A.** Specific features of joint space in patients with physiological occlusion on computed tomogram head image // *Archiv EuroMedica.* 2019. Vol. 9; 2: 182–183. <https://doi.org/10.35630/2199-885X/2019/9/2/182>
47. The revised Ghent nosology for the Marfan syndrome / B. L. Loeys, H. C. Dietz, A. C. Braverman et al. // *J. Med. Genet.* 2010. Vol. 47 (7). P. 476–485. DOI: 10.1136/jmg.2009.072785